Available online at www.sciencedirect.com
ScienceDirect
Renewable and Sustainable Energy Reviews
12 (2008) 999–1031
RENEWABLE & SUSTAINABLE ENERGY REVIEWS
www.elsevier.com/locate/rser

Review of mathematical modeling on latent heat thermal energy storage systems using phase-change material

Prashant Verma[a], Varun[a], S.K. Singal[b,*]

[a]Department of Mechanical Engineering, Ram Ganga Vihar, Phase-2, Moradabad 244001, UP, India
[b]Alternate Hydro-Energy Center, Indian Institute of Technology, Roorkee 247667, UP, India

Received 17 April 2006; received in revised form 19 July 2006; accepted 27 November 2006

Abstract

Mathematical modeling of a latent heat thermal energy storage system (LHTES) was used for the optimum material selection and to assist in the optimal designing of the systems. In this paper, two types of models are mainly discussed, on the basis of first law and second law of thermodynamics. The important characteristics of different models and their assumptions used are presented and discussed, the experimental validation of some models are also presented.

Keywords: Latent heat; Modeling; Storage system; Phase-change material

Contents

*Corresponding author. Tel.: +91 1332 285 167; fax: +91 1332 273 517.
E-mail address: sunilfah@iitr.ernet.in (S.K. Singal).

1364-0321/$ - see front matter
doi:10.1016/j.rser.2006.11.002

Nomenclature

A	area of cross-section of duct
A_f	passage cross-sectional area (m^2)
A_n	surface area of boundary node (m^2)
Ar	$(\rho_l - \rho_s)/\rho_s g r_o^3/v^2$ (dimensionless)
a	width of heat exchanger
b	air gap
Bi	Biot number
C	effective heat capacity
C_{pa}	actual specific heat
C_p	specific heat (J/kg K)
c_a	heat capacity of air (1007 J/kg K)
c_l	sensible heat of liquid PCM (J/m^3)
c_s	sensible heat of solid PCM (J/m^3)
D	diameter of tube
f	proportional constant for Φ versus τ
Fo	Fourier number
H	enthalpy
h	sensible volumetric enthalpy (J/m^3)
h_c	convection heat-transfer coefficient
h_f	latent heat of fusion (J/kg)
K	thermal conductivity of PCM (W/m °C)
L	length of heat exchanger
L_c	length of cylinder (m)
ℓ	length of storage system (m)
l_c	characteristic length of PCM capsule (m)
m	mass flow rate (kg/s)
NTU	number of transfer units
N_s	entropy generation number
P	perimeter of heat exchanger = $2a$
Pr	Prandtl number
Q	calculated power of the heat exchanger
Q_a	actual heat-transfer rate
q''	heat flux (W/m^2)
Ra	Rayleigh number
$R_{c,inn}$	inner radius of cylinder (m)
$R_{c,out}$	outer radius of cylinder (m)
r_i	radius of the tube
r_o	radius of PCM cylinder
S	local melted layer thickness (m)
s	separation parameter
Ste	Stefan number
S_o	melted layer thickness at the bottom (m)
$(Sg)_s$	specific entropy generation in heat storage process (J/kg K)
$(Sg)_r$	specific entropy generation in heat retrieval process (J/kg K)

T	temperature (°C)
t	time (s)
T_a	ambient temperature (K)
T_{sat}	saturation temperature
T_m	PCM melting temperature
T_{PCM}	temperature in PCM
$T(x)$	temperature at coordinate x
T_o	inlet air temperature
T_∞	coolant temperature
T_{ci}	source temperature of hot fluid
u	ratio of x/δ
U_p	heat-transfer coefficient between middle of PCM and air
v	velocity (m/s)
V_o	capsule volume (m^3)
V_p	solid PCM volume (m^3)
$\bar{V}_p$	V_p/V_o, dimensionless solid PCM volume
V_{tank}	inside volume of tank (m^3)
W	exergy rate
W_s	availability of operating fluid flowing to system during heat storage process (J)
W_r	availability of operating fluid flowing to system during heat retrieval process (J)
x	length coordinate
x_w	distance from the wall (m)
x, y, z, r	space coordinate
Δ_{mi}	temperature difference (T_{wv}–T_i) (K)
Δ_{wm}	temperature difference (T_{wv}–T_m) (K)
θ_s	dimensionless capsule surface temperature $[(T_s–T_{in})/T_m–T_{in})]$
α_p	fictive heat-transfer coefficient
ρ_a	density of air (1.20 kg/m^3)
θ	dimensionless temperature (T/T_a)
θ_{di}	dimensionless heat-transfer fluid inlet temperature for the discharge process
θ_{do}	dimensionless heat-transfer fluid outlet temperature for the discharge process
θ_m	dimensionless melting temperature of the PCM for the single PCM case

Greek letters

τ	dimensional time
λ	proportionality parameter of S_o versus t
α	thermal diffusivity (m^2/s)
ψ	second law efficiency
ρ	density of PCM (kg/m^3)
ϕ	inclination angle of the solid–liquid interface
ϖ	dimensionless exergy rate
δ	solid layer thickness (m)
β	exergy efficiency

Subscripts

a	air
a_o	air outlet
a_i	air inlet
c	charge process
d	discharge process
F	fluid
i	initial condition
in	inlet
l	liquid
o	outside
out	outgoing
r	ratio of solid–liquid properties
s	solid
T	total
t	tube
w	container wall
w_v	vertical heated wall

Superscripts

F	fluid
P	PCM
1	storage system consisting of single PCM

1. Introduction

Storage of thermal energy is very important in many engineering applications. Efforts of rational and effective energy management as well as environmental considerations increased the interest in utilizing renewable energy sources, especially solar energy. Because of discrepancy between the energy supply and demand in solar heating applications, a thermal energy storage device has to be used. Similar problems arise for waste heat recovery systems where the waste heat availability and utilization periods are different. Heat storage can also be applied in most types of buildings where heating needs are significant and electricity rates allow heat storage to be competitive with other forms of heating.

The basic types of thermal energy storage techniques can be described as sensible heat storage and latent heat storage. In sensible heat storage, temperature of the storage material varies with the amount of energy stored for example in solar heating systems water is used for heat storage in liquid-based systems, while a rock bed is used for air-based systems. In the application of load leveling heat is usually stored in refractory bricks storage heater [1] (known as night storage heater), storage in salty water (solar pond), storage in petroleum-based oils and molten salts such as Therminol and Caloria-HT [2] oils and sodium hydroxide salt [1], liquid metals are also used as sensible heat storage media and metals such as aluminum, magnesium and zinc can also be used for energy

storage. Latent heat storage is a particularly attractive technique since it provides a high-energy storage density and has the capacity to store as latent heat of fusion at a constant temperature corresponding to the phase transition temperature of the phase-change materials (PCMs). For example in the case of water, 80 times as much energy is required to melt 1 kg of ice as to raise the temperature of 1 kg of water by 1 °C. This means that a much smaller weight and volume of material is needed to store a certain amount of energy.

Table 1 shows a comparison between the sensible heat storage using a rock bed and water tank and also shows the latent heat storage using organic and non-organic compounds. The advantage of the latent heat over the sensible heat is clear from the comparison of the volume and mass of the storage unit required for storing a certain amount of heat. It is also clear from Table 1 that inorganic compounds, such as hydrated salts, have a higher volumetric thermal storage density than the most of the organic compounds due to their higher latent heat and density. The various PCMs are generally divided into three main groups: organic, inorganic and eutectics of organic and/or inorganic compounds. Organic compounds present several advantages such as non-corrosiveness, low or no under cooling, possess chemical and thermal stability [3], ability of congruent melting, self-nucleating properties and compatibility with conventional materials of construction. Subgroups of organic compounds include paraffin and non-paraffin organics. Technical grade paraffin has been extensively used as heat storage materials due to wide melting/solidification temperature ranges and has a relatively high latent heat capacity. They also have no subcooling effects during the solidification as well as small volume change during the phase-change process. They are chemically stable, non-toxic and non-corrosive over an extended storage period. Widely used non-paraffin organics, as latent heat storage materials are fatty acids like lauric, myristic, palmitic and stearic acid. Their advantages are a possibility for reproducible melting and solidification behavior and little or no subcooling effects. Disadvantages of organic compounds include lower phase-change enthalpy, low thermal conductivity and inflammability.

Inorganic compounds include salt hydrates, salts, metals and alloys. A number of salt hydrates such as sodium sulfate decahydrate (Glauber's salt), calcium chloride hexahydrate, sodium thiosulfate pentahydrate, sodium acetate trihydrate and barium hydroxide octahydrate, were investigated largely because of their low cost [1,4–8]. The main advantages of inorganic compounds are a high volumetric latent heat storage capacity, often twice the capacity of organic compounds and high thermal conductivity.

Table 1
Comparison between the different methods of heat storage [1]

Property	Rock	Water	Organic PCM	Inorganic PCM
Density (kg/m^3)	2240	1000	800	1600
Specific heat (kJ/kg)	1.0	4.2	2.0	2.0
Latent heat (kJ/kg)	—	—	190	230
Latent heat (kJ/m^3)	—	—	152	368
Storage mass for 10^6 J (kg)	67,000	16,000	5300	4350
Storage volume for 10^6 J (m^3)	30	16	6.6	2.7
Relative storage mass	15	4	1.25	1.0
Relative storage volume	11	6	2.5	1.0

Major problems with most of the salt hydrates are supercooling, phase segregation, corrosion and lack of thermal stability. Supercooling in several salt hydrates has been prevented by adding nucleating agents or by promoting nucleation by rough container walls or using the cold finger technique [5,6,9,10]. To prevent phase segregation, several techniques, such as use of thickening agents, rotating storage devices and direct contact heat transfer have been used [10,11]. Although, an overview of PCMs used in low thermal energy systems has been given by Abhat [12], Zalba et al. [13] and Farid et al. [14]. Tables 2 and 3 list thermo-physical properties of some organic and inorganic PCMs.

Eutectics are mixtures of two or more salts which have definite melting–freezing points. Their behavior is analogous to congruent melting salt hydrates and has great potential for thermal energy storage application. A large number of eutectics of inorganic and organic compounds have been reported in [1,10,15] and they can be classified as inorganic eutectics, organic eutectics and organic–inorganic eutectics. Some of the eutectics are listed in Tables 4 and 5.

Table 2
Inorganic substances with potential use as PCM

Compound	Melting temperature (°C)	Heat of fusion (kJ/kg)	Thermal conductivity (W/m K)	Density (kg/m^3)
$KF\cdot 4H_2O$ [12,13,17,18]	18.5	231	n.a.	1447 (liquid, 20 °C) 1455 (solid, 18 °C) 1480
$Mn(NO_3)_2\cdot 6H_2O$ [19,20]	25.8	125.9	n.a.	1738 (liquid, 20 °C) 1728 (liquid, 40 °C) 1795 (solid, 5 °C)
$CaCl_2\cdot 6H_2O$ [4,12,13,17,18,21,22,23]	29	190.8	0.540 (liquid, 38.7 °C)	1562 (liquid, 32 °C)
	29.2	171	0.561 (liquid, 61.2 °C)	1496 (liquid)
	29.6	174.4	1.088 (solid, 23 °C)	1802 (solid, 24 °C)
	30	192		1710 (solid, 25 °C)
$Na_2SO_4\cdot 10H_2O$ [4,12,13,17,18]	32.4	254	0.544	1485 (solid)
	32	251.1		1458
$Na_2HPO_4\cdot 12H_2O$ [4,13,17,18,22]	35.5	265	n.a.	1522
	36	280		
	35	281		
$Mg(NO_3)_2\cdot 6H_2O$ [13,17,21,22,23]	89	162.8	0.490 (liquid, 95 °C)	1550 (liquid, 94 °C)
	90	149.5	0.502 (liquid, 110 °C)	1636 (solid, 25 °C)
$MgCl_2$ [13]	714	452	n.a.	2140
NaCl [13]	800	492	5	2160

n.a.: not available.

Table 3
Organic substances with potential use as PCM

Compound	Melting temperature (°C)	Heat of fusion (kJ/kg)	Thermal conductivity (W/m K)	Density (kg/m^3)
Paraffin C_{16}–C_{18} [13]	20–22	152	n.a.	n.a.
Paraffin C_{13}–C_{24} [12]	22–24	189	0.21 (solid)	0.760 (liquid, 70 °C) 0.990 (solid, 20 °C)
Poly-glycol E600 [21,23]	22 n.a.	127.2 n.a.	0.189(liquid, 38.6 °C) 0.187 (liquid, 67 °C)	1126 (liquid, 25 °C) 1232 (solid, 4 °C)
Paraffin C_{18} [12,24]	28 n.a. 27.5	244 n.a. 243.5	0.148 (liquid, 40 °C) 0.15 (solid) [1] 0.358 (solid, 25 °C)	0.774 (liquid, 70 °C) n.a. 0.814 (solid, 20 °C)
Paraffin wax [13,21,23]	64	173.6	0.167(liquid, 63.5 °C) 0.346 (solid, 33.6 °C) 0.339 (solid, 45.7 °C)	790 (liquid, 65 °C) 916 (solid, 24 °C)
Naphthalene [21,23]	80	147.7	0.132 (liquid, 83.8 °C) 0.341 (solid, 49.9 °C)	976 (liquid, 84 °C) 1145 (solid, 20 °C)

n.a.: not available.

Table 4
Inorganic eutectics with potential use as PCM

Compound	Melting temperature (°C)	Heat of fusion (kJ/kg)	Thermal conductivity (W/m K)	Density (kg/ m^3)
66.6% $CaCl_2 \cdot 6H_2O$ + 33.3% $MgCl_2 \cdot 6H_2O$ [13]	25	127	n.a.	1590
48% $CaCl_2$ + 4.3% NaCl + 0.4% KCl + 47.3 $\cdot$ H_2O [12,13]	26.8	188	n.a.	1640
61.5% $Mg(NO_3)_2 \cdot 6H_2O$ + 38.5% NH_4NO_3 [23]	52	125.5	0.494 (liquid, 65 °C) 0.515 (liquid, 88 °C) 0.552 (solid, 36 °C)	1515(liquid, 65 °C) 1596(solid, 20 °C)
11.8% NaF + 54.3% KF + 26.6% LiF + 7.3% MgF_2 [25]	449	n.a.	n.a.	2160 (liquid)
60% $Na(CH_3COO) \cdot 3H_2O$ + 40% $CO(NH_2)_2$ [26,20]	31.5 30	226 200.5	n.a n.a	n.a n.a

% in weight.
n.a.: not available.

Table 5
Organic eutectics with potential use as PCM

Compound	Melting temperature (°C)	Heat of fusion (kJ/kg)	Thermal conductivity (W/m K)
37.5% Urea + 63.5 acetamide [12]	53	n.a.	n.a.
67.1% Napthalene + 32.9% benzoic acid [23]	67	123.4	0.136 (liquid, 78.5 °C) 0.130 (liquid, 100 °C) 0.282 (solid, 38 °C) 0.257 (solid, 52 °C)
Lauric–capric acid [1]	18	120	n.a.
Lauric–palmitic acid [1]	33	145	n.a.
Lauric–stearic acid [1]	34	150	n.a.

% in weight.
n.a.: not available.

Successful utilization of PCM heat-transfer media depends on developing means of containment or encapsulation. Several different techniques [16] have been studied for encapsulating heat sink chemicals in plastic or metal matrices. These can be divided into three categories on the basis of the size of the encapsulated particle [16].

(i) Microencapsulation of emulsion-sized particles.
(ii) Encapsulation of granules.
(iii) Macroencapsulation of large blocks or shapes.

Encapsulation results in the improvement of the physical and chemical stability of the heat sink material, fabrication of encapsulated structures would facilitate production of modular heat storage units and useful structural or architectural materials would be developed. The most cost-effective containers are plastic bottles and tin-plated food cans [7]. However, corrosion could lead to disastrous consequences if internal and external lacquer finishes are not applied properly to the mild steel can.

2. Review of mathematical/numerical modeling of latent heat thermal energy storage

The use of exergy analysis is very important in developing a good understanding of the thermodynamic behavior of thermal energy storage systems because it clearly takes into account the loss of availability and temperature of heat in storage applications, and hence it more correctly reflects the thermodynamic and economic value of the storage operation [27]. An analysis, which is solely dependent on the first law of thermodynamics, is inadequate as a measure of the energy storage because it does not consider the effect of time duration through which heat is supplied and the temperature of the surroundings. The energy analysis might produce a workable design, but not necessarily one with the highest possible thermodynamic efficiency [28]. In contrast an analysis consideration leads to optimal design operation of thermal system. Bejan [29] defined the optimal thermal system as the least irreversible system a designer can develop using thermal design techniques that are based on minimization of entropy generation. Bejan [27] calculated the minimum entropy generation number as a function of the different operation and design variables for only the thermal energy storage process. Although Krane [28] modified Bejan's analysis

by accounting for both the heat storage and retrieval process and later [30] applied the techniques of second law analysis to optimize the design of thermal energy storage system with Joulean heaters.

Adebiyi et al. [31] reported that none of the availability analyses cited have treated thermal energy storage systems that utilize PCM. However, the study showed that elimination of the time periods required to heat or to cool the storage material above or below the melting temperature, respectively, can improve the second law efficiency of the system. The analysis of heat-transfer problems in melting and solidification process, called moving boundary problems in scientific literature, is especially complicated due to the fact that the solid–liquid boundary moves depending on the speed at which the latent heat is absorbed or lost at the boundary, so that the position of the boundary is not known a priori and forms part of the solution. When the substance that solidifies is pure, the solidification occurs at single temperature, while in the opposite case such as with mixtures alloys and impure materials, the solidification takes place over a range of temperatures and therefore there appears a two-phase zone (mushy region) between the solid and liquid zones. In the latter case, it is appropriate to consider the energy equation in terms of enthalpy, which if the advective movements in the inner of the liquid are disregarded, is expressed mathematically as

$$\rho \frac{\partial h}{\partial t} = \vec{\nabla}(\vec{K}\nabla\vec{T}). \tag{1}$$

Solution of this equation requires knowledge of the enthalpy temperature functional dependency; similarly it is necessary to know the function relating the thermal conductivity and the temperature. The strength of this method lies as the equation is directly applicable to the three phases, the temperature is determined at each point and the value of thermo-physical properties can be evaluated, and finally according to the temperature field, it is possible to ascertain the position of two boundaries if so desired, although as indicated above this is not necessary. Shamsunder et al. [32] demonstrated the equivalence between the energy conservation equation applied in the three zones (solid, liquid and solid/liquid) and the enthalpy model. They analyzed a specific problem associated with a solar energy storage unit. Multi-dimensional conduction phase-change analysis is performed via enthalpy model employing a fully implicit finite-difference scheme to solve for solidification in a convectively cooled square container. In the present paper, the mathematical/numerical modeling done by various researchers, considering the analyses on the basis of first law of thermodynamics or enthalpy approach and second law of thermodynamics has been discussed.

3. Modeling based on first law of thermodynamics

Shamsundar et al. [32] analyzed a specific problem associated with a solar energy storage unit. Multi-dimensional conduction phase-change analysis is performed via enthalpy model employing a fully implicit finite-difference scheme to solve for solidification in a convectively cooled square container. Following assumptions were made in the analysis:

- PCM is initially in the liquid state at its saturation temperature.
- Coolant temperature and convective heat-transfer coefficient are uniform along the surface and constant with time.

- The container wall has negligible thermal resistance and heat capacity.
- Aside from enthalpy, the properties of PCM are assumed to be independent of temperature.

The implicit scheme was selected because of its ability to accommodate a wide range of Stefan number (*Ste*). After the establishment of accuracy, the solution method was used to obtain results for surface integrated heat-transfer rates; boundary temperatures solidified fraction and interface position all as function of the time. The product *Ste*–*Fo*, rather than the Fourier number *Fo*, is used because it correlates the results for the various values of *Ste*. After analysis following results were obtained:

For the distribution of heat flux on cooled surface of PCM for Biot number $Bi = 0.1$, 1.0 and 10 and $Ste = 0.10$, 0.05 and 0.01 as the freezing progresses, the heat flux decreases faster at the corner of container than at the line of symmetry. With respect to the effect of *Bi*, it may be noted that at the same level of dimensionless heat flux, the region of spatial uniformity is larger at higher *Bi*, with a correspondingly steeper drop off near the corner. At comparable values of the frozen fraction, smaller values of dimensionless heat flux are in evidence at higher *Bi* values.

$$\text{Dimensionless heat flux} = \frac{T_{\mathrm{w}} - T_{\infty}}{T_{\mathrm{sat}} - T_{\infty}}. \tag{2}$$

As far as thermal storage is concerned to obtain a steady rate of energy extraction small volumes of *Bi* should be employed. As the Biot number increases the freezing rate varies more and more with time, starting with the highest rate at the beginning and then decreasing continuously till the end. As the freezing progresses, the propagation of the two-dimensionality into the growing solid region causes the interface to be more curved and near the end of solidification, there is a significant effect of *Ste*.

Hamdan et al. [33] presented a model as illustrated in Fig. 1 to predict the melted fraction of the PCM and hence the amount of energy stored. Figure shows the rectangular enclosure whose sides are well insulated except the left vertical side along which heat is supplied. The enclosure contains a pure PCM, which is assumed to be initially in solid phase and at an initial temperature (T_{i}). As heat is supplied through the left side, melting process starts when the temperature of the solid layer adjacent to the heated side exceeds the melting temperature of the material (T_{m}). The solid–liquid interface propagates in the positive direction of x coordinates. The rate of melting depends essentially on the properties of the material, such as thermal diffusivity, viscosity, conductivity, latent heat of fusion and specific heat. The model follows a two-dimensional melting process of a solid PCM considering convection as a dominant mode with in the melt region, except with in the layer very close to the solid boundary in which only conduction is assumed to take place, besides this melting of PCM also takes into account the inclination of solid–liquid interface. For the evaluation of interface propagation the equation used was as outlined by Elwerr [34] to obtain

$$(Ra^{1/5}\rho_{\mathrm{r}}/Ste)\int \frac{\partial S}{\partial \tau}\,\mathrm{d}y = (4/25\cos\phi)[2\Delta_{\mathrm{wm}}^{5/4}(\cos\phi)^{2/3} - (3K_{\mathrm{r}}\Delta_{\mathrm{mi}}/\sqrt{\alpha_{\mathrm{r}}\tau})]. \tag{3}$$

For the evaluation of the interface inclination equation used is

$$\frac{\mathrm{d}\phi}{\mathrm{d}\tau} = [2(\cos\,\phi)^2(4Ste/(25(Ra)^{1/5}\rho_{\mathrm{r}}\cos\phi))] \times [2(Ra)^{1/4}(\cos\phi)^{2/3} - (3K_{\mathrm{r}}\Delta_{\mathrm{mi}}/\sqrt{\alpha_{\mathrm{r}}\tau})] - (\lambda/\sqrt{2}). \tag{4}$$

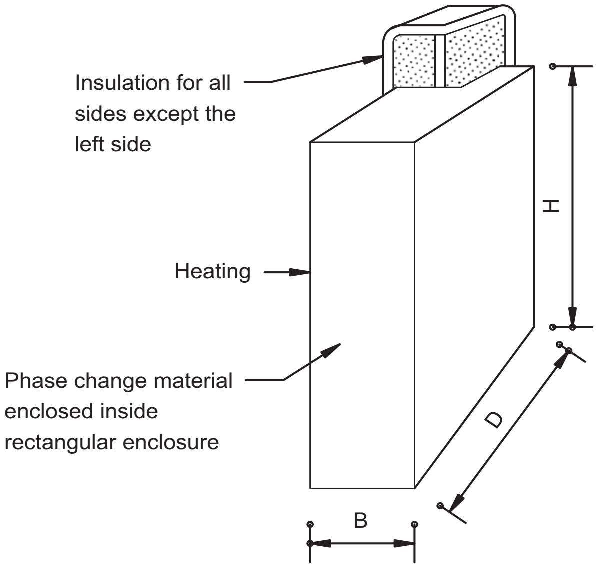


Fig. 1. A scheme for the physical model.

By Bernard et al. [35] ϕ may be approximated as

$$\phi = f\tau \ \ (\text{for} \ \ \tau > \tau_o). \tag{5}$$

Upon substitution in above equation, it may be integrated and value for f may be estimated by trial and error. The results obtained such as melted fraction of PCM shows a good agreement with the experimental work carried out by Bernard et al. [35], who used *n*-octadecane as a PCM and numerical work done by Webb and Viskanta [36] taking pure gallium as PCM. However, the comparison of position and inclination of the interface between this work and experimental work of Bernard et al. [35] is in good agreement in early stages of melting but deviates from the analysis as the height of the employed model increases. This deviation is attributed to the assumption of considering inclination angle Φ independent of height. Further, the results obtained shows that the analysis gives more rapid interface propagation than the experimental data due to the assumption that the walls of the enclosures are all adiabatic except the heated one, while the experimental data are not based on this assumption.

Kurkulu et al. [37] developed a mathematical model for the prediction of the thermal performance of a square cross-sectioned PCM store as shown in Fig. 2 containing 1 m long and 38 mm diameter polypropylene tube. This model was based on energy balance or the conservation of energy principle. The model was analyzed by considering the effect of thermo-physical properties of PCM as well as tube, the PCM used was a mixture of sodium sulfate and sodium chloride salts and water together with additives to prevent supercooling and phase segregation and air is used as a heat-transfer fluid (HTF). The basic energy equation is employed to a control volume about an interior node after dividing the tube into 5 volumes and 25 equal length elements. To simplify the analysis following assumptions were made:

- The phases are homogeneous.
- The variation of thermo-physical properties with temperature with in any phase was ignored due to smaller temperature variation.

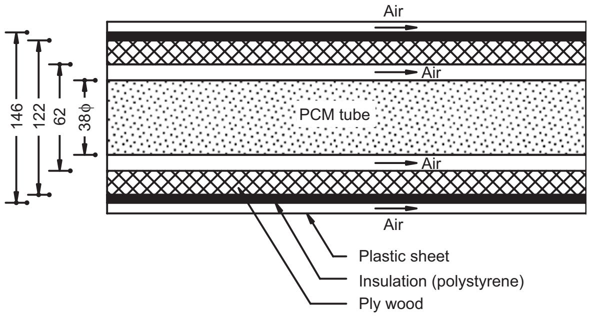


Fig. 2. Schematic and dimensions of the experimental store.

- Convection heat transfer does not occur in liquid phase.
- Supercooling does not take place.
- Heat loss or gain from the store is neglected.

The volume node that involved freezing here was the one, which was adjacent to a solid node on one side and to a liquid node on the other side. The other nodes were assumed to be either completely liquid or completely solid. Thus, accounting for changes in thermal energy storage, a general form of the energy balance equation can be expressed as follows:

$$Q_\varepsilon - Q_{\text{out}} = Q_{\text{st}}. \tag{6}$$

Experimental setup consists of an air conditioning laboratory unit was used to supply air at controlled and desired temperature to the inlet of PCM store. In the experiments the required air mass flow rate was provided by the variable speed centrifugal fan on the air conditioning unit, air inlet temperatures of 11, 14 and 17 °C and air mass flow rates of 0.0033, 0.0058 and 0.0083 kg/s were used. The experimental heat-transfer rates between the PCM tube and air were calculated from the equation below:

$$Q_{\text{a}} = mC_{p\text{a}}(T_{\text{ao}} - T_{\text{ai}}). \tag{7}$$

The numerical mathematical data was first validated with experimental data. The model was set up to calculate the temperature of air and that of the PCM at the formerly defined volume nodes. The *F*-value that is the % of energy that was released to decrease the temperature of PCM whilst freezing, was found to be 3.8%. The final value of *F* was defined after several trial and error computations by the model and then by comparing the predicted temperature values with the experimental ones. The *F*-value, which gives the best agreement with the experimental complete melting time of the PCM, was then chosen. Comparison of the observed and predicted temperature data for air mass flow rates of 0.0033 and 0.0058 kg/s at air inlet temperature of 11 °C shows a good agreement. It is found that as the air mass flow rate increased or the air inlet temperature decreased the phase change (or complete freezing) time of the PCM decreased and the amount of energy used in increasing the temperature of the PCM at any time during the phase change is predicted to be about 3.5% of the total energy stored. Moreover, sensitivity analysis of the model shows that increase in time increment at a particular mass flow rate and air inlet temperature has no significant effect on the calculation output; however, change in

convective surface heat-transfer coefficient has significant effect on the model for a volume element with constant dimensions.

Esen et al. [38] developed a model to investigate theoretically the performance of a solar-assisted cylindrical energy storage tank which was considered a part of domestic heating system. In the tank, the PCM is packed in cylinders and HTF flows parallel to it. The PCM considered are calcium chloride hexahydrate ($CaCl_2 \cdot 6H_2O$), Paraffin wax (P-116), $Na_2SO_4 \cdot 10H_2O$ and paraffin. Fig. 3 shows the configuration chosen for the storage vessel. It consists of a vessel packed in the vertical direction with cylindrical tubes. Besides the PCM, the latent heat storage system contains a fluid for the heat transfer towards or from the heat-storage material. The PCM and the HTF are separated. The shape of the packing of the PCM and the HTF is of a cylindrical in nature. In this study, we consider a configuration of packing of the storage material, which is a vessel, packed in the vertical direction with cylindrical tubes; the PCM is inside the tubes and the HTF flows parallel to it. We decide to describe the vessel as follows.

For the model, we assume that the HTF, which is surrounding the cylinders, is situated in cylinder jackets all round the tubes. Of course, the volume of all these cylinder jackets together is equal to the fluid volume in the real storage tank. The density of the packing is the same anywhere in the tank. To have as much PCM as possible enclosed within a tank of a certain volume, we shall mostly aim at a close packing of the cylinders. However, again, we notice that this is not necessary. The main objectives of the study were to develop a model of phase-change energy storage that considers the heat loss from the storage unit, the axial and radial conduction in the storage material and the local film temperature difference between the fluid and the PCM. The model is based on enthalpy method and the resulting sets of equations were solved by Gauss–Seidel iteration process. Selected

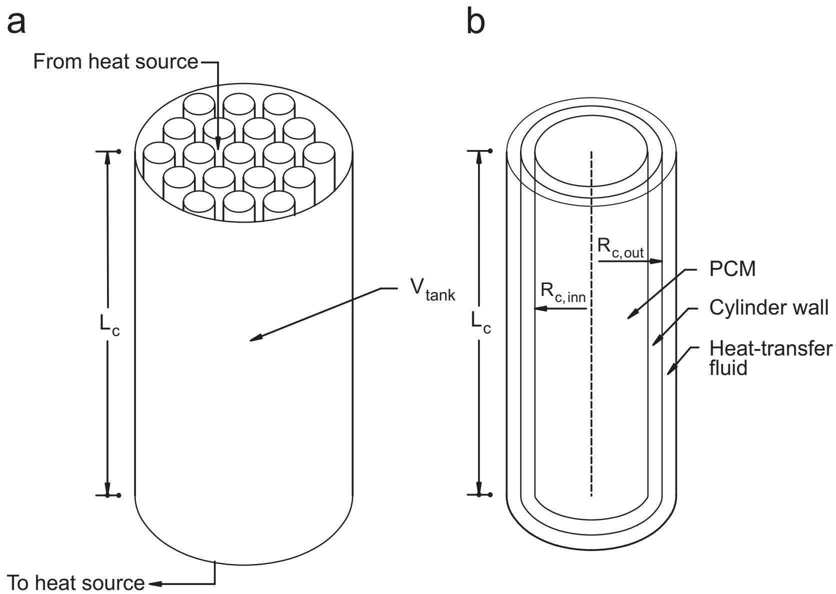


Fig. 3. (a) The cylinder-packed vessel and (b) the model for one cylinder.

computer simulations are drawn versus some parameters (inner radius of cylinder, mass flux of HTF flowing from heat source to tank and temperature of HTF flowing from heat source to tank) of the model, and the heat storage capacities of different PCMs, which can be used as heat storage materials for domestic heating by heat pumps, were determined and compared.

The performance of cylindrical energy storage tank was determined by Transient Simulation Programme [39] and Computer simulations [40] shows the variation of stored energy in the PCM with time for various PCM's at different values of mass flow rate and inlet HTF temperature. The result shows that the stored energy becomes bigger at a given time as the mass flow rate or inlet HTF temperature increases. It is seen that as the radius of PCM cylinder increases at a constant mass of $CaCl_2 \cdot 6H_2O$, the whole $CaCl_2 \cdot 6H_2O$ melting time increases, and for more energy storage appropriate cylinder wall materials and dimensions should be selected, such as bigger thermal conductivity and small radius. The numerical predictions were validated with experimental data.

Gong et al. [41] developed a finite-element model to simulate the cyclic thermal process occurring in a shell and tube latent heat thermal storage exchanger as shown in Fig. 4. This exchanger consists of a tube which is surrounded by an external co-axial cylinder made up of PCM which is a mixture of 80.5% LiF and 19.5% CaF_2 where as the HTF considered was a mixture of He/Xe. The objective of this model is to investigate the characteristics of two operation modes, which are named mode 1 and mode 2. In mode 1 the hot and cold fluids (for charge and discharge process, respectively) are introduced from the same end of the tube where as in mode 2 the hot and cold fluids are introduced from different ends of the tube. It should be noted that the selection of the PCM and the HTF is not made for a specific application. The assumptions made for the mathematical description of the model are:

- The heat-transfer fluid is incompressible and viscous dissipation is negligible.
- The fluid flow is radially uniform and the axial velocity is an independent parameter.
- Thermal losses through the outer wall of the PCM are negligible.
- Heat transfer in the PCM is conduction controlled.
- The densities of the solid and liquid phases of the PCM are equal.

Based on the above assumptions, the governing equation for energy transfer in the fluid is

$$\rho_F c_F \left(\frac{\partial T^F}{\partial t} + v \frac{\partial T^F}{\partial x} \right) = \frac{4h_c}{D}(T^P - T^F) + K_F \frac{\partial^2 T^F}{\partial x^2} \tag{8}$$

and the equation for energy transfer in the PCM is

$$\frac{\partial H^P}{\partial t} = \left(\frac{1}{r} \right) \frac{\partial}{\partial r} \left(K_P r \frac{\partial T^P}{\partial r} \right) + \frac{\partial}{\partial x} \left(K_P \frac{\partial T^P}{\partial x} \right). \tag{9}$$

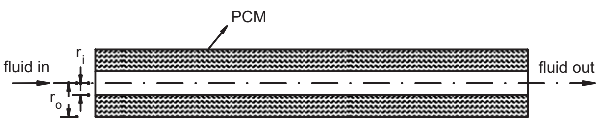


Fig. 4. Physical model [41].

The instantaneous temperature distributions in the PCM are obtained using standard Galerkin finite-element method [42] and a three time-level scheme [43] incorporating lumped heat capacity [44] is used to accomplish the time discretization of equation. The magnitude of the cumulative energy charged or discharged Q, is calculated as a function of time for each charge or discharge period. This calculation is made by computing the enthalpy of the PCM at each time increment, using the solid PCM at its fusion temperature as the reference state, and then subtracting the enthalpy of the PCM at the beginning of the period. The value of Q is zero at the beginning of a period and increases over a period towards Q_r, the cumulative energy charged or discharged in the period. To prove the validity of the numerical model, an overall energy balance is performed at each time step. The enthalpy stored in the PCM is compared with the thermal-energy loss by the heat-transfer fluid. It was found that the difference never exceeds 0.1%. Computations are carried out to simulate the cyclic heat-transfer processes of energy charge/discharge to investigate the effects of the two operation modes on the performance of the storage exchanger.

For the computation 30×10 elements in the PCM region and correspondingly 30 elements in the fluid with a time step of 2 s were used for the computation, taking both the accuracy requirement and computing time into consideration. Dynamic simulations are carried out until a steady reproducible state (SRS) is reached. In this state, the transient thermal process occurs repeatedly from cycle to cycle, and the temperature fields in the PCM and the fluid, as well as the cumulative energy charged/discharged in each charge or discharge period, are the same from cycle to cycle. Analyses show that the energy charged/discharged in a cycle using mode 1 is 5.0% more than when using mode 2. This means that the energy charge/discharge rate can be 5.0% faster when using mode 1. The energy charged/discharged rate is faster when using mode 1 because it is known that the temperature difference for heat transfer between the fluid and the PCM is higher in the fluid inlet than in the outlet. The larger the temperature difference, the more deeply the phase-change interface penetrates into the PCM. In the energy-charge process, the liquid–solid phase-change interface penetrates more deeply into the PCM in the fluid-inlet region than in the outlet region. In the energy-discharge process, similar phenomena occur. If the hot fluid is introduced from the left end of the tube in the energy-charge process, and the cold fluid is introduced from the right end in the energy-discharge process, supercooling of the PCM becomes very significant in the inlet region of the cold fluid (the right end of the tube). This is particularly evident during the final stage of the process, since the depth of the PCM melted in the energy-charge process is much smaller at the right end than at the left end of the tube. This supercooling causes heat transfer between the fluid and the PCM to deteriorate. It is known that the melted depth of PCM in the fluid-inlet region (left end) of the energy-charge process is larger. If the cold fluid is introduced from the same end (left end) of the tube in the energy-discharge process, the penetration depth of the solid–liquid phase-change interface is also larger at the left end of the tube. This matches the larger depth melted in the energy-charge process. Therefore, supercooling of the PCM does not occur in the fluid-inlet region, and heat transfer between the heat-transfer fluid and the PCM does not deteriorate. This explains reason for the energy charge/discharge rate is larger in mode 1 than mode 2.

Between the two operations modes assuming the duration of charge and discharge process same it is found that (a) the enhancement of the cumulative energy charged/discharged in a cycle at SRS slightly increases with an increase in the fluid flow rates. This

result indicates that no matter how the fluid flow rate changes, the enhancement of the cumulative energy charge/discharge rate is almost the same (b) enhancement of the cumulative energy charged/discharged in a cycle at SRS decreases with an increase of the inlet temperature of the heat-transfer fluid. This means that the smaller the Stefan number of the phase-change heat transfer in the PCM, the larger the enhancement of the energy charge/discharge rate when using mode 1 than when using mode 2. From this result it is clearly seen that it is more unfavorable to use mode 2 of operation, particularly at small temperature differences, where as the effect of duration of the charge/discharge period on energy charge/discharge rate shows that the enhancement of the cumulative energy charged/discharged in a cycle at SRS decreases with an increase in the duration of a period. The shorter the duration of the charge/discharge time, the smaller the superheating and supercooling effects for mode 1, and the larger the enhancement of the energy charge/discharge rate. It can be concluded that introducing the hot and cold fluid from the same end of the storage exchanger is more desirable than introducing the hot and cold fluid from different ends of the storage exchanger.

Costa et al. [45] designed and fabricated a system to take advantage of the off-peak electrical energy for space heating by using *n*-octadecane as PCM and aluminum as a container. The schematic diagram of the system is shown in Fig. 5. The system consists of seven aluminum rectangular containers for the PCM, and the inside dimensions of each container are $6.0\,cm \times 6.0\,cm \times 25.4\,cm$. The thickness of the used container material is 2 mm. It will act as a fin and will help to enhance the rate of heat transfer in the PCM. The total mass of the PCM, which can be filled, is 3.9 kg. On one side of the PCM containers, 10 rectangular aluminum tubes, each $2.5\,cm \times 1.25\,cm \times 44.0\,cm$ (exterior dimensions), have been fixed for fluid flow and to withdraw the stored heat whenever required. To melt the PCM, an electric heater has been provided on the other side of the PCM containers. The whole system is kept in a well-insulated box to provide adiabatic conditions. *n*-Octadecane has been chosen as a PCM because the liquid is transparent, and it has a relatively low and uniform melting temperature.

The objective of the design was to study the thermal performance of the system and the effect of natural convection during the melting and solidification process. The thermal performance of storage system has been analyzed using an enthalpy formulation and a fully implicit finite-difference method [46,47]. The model has been developed to predict the one-dimensional considering conduction and convection without fins and two-dimensional considering conduction only with fins behavior of latent heat energy storage system. To analyze the system authors has made the following assumptions is his study:

- The thermo-physical properties of the PCM and fin material are independent of temperature. However, they are different for the solid and liquid phases of PCM.
- The PCM is initially in the solid phase, homogeneous and isotropic and PCM temperature is at a certain temperature below its melting point.
- All PCM subunits are identical and independent of each other.

For code validation to test the accuracy of computer program, one-dimensional and two-dimensional numerical tests have been performed. To investigate the accuracy of one-dimensional program the one-dimensional test problem used by Voller [46] and Goodrich [48] was introduced. The results obtained show excellent agreement with the results

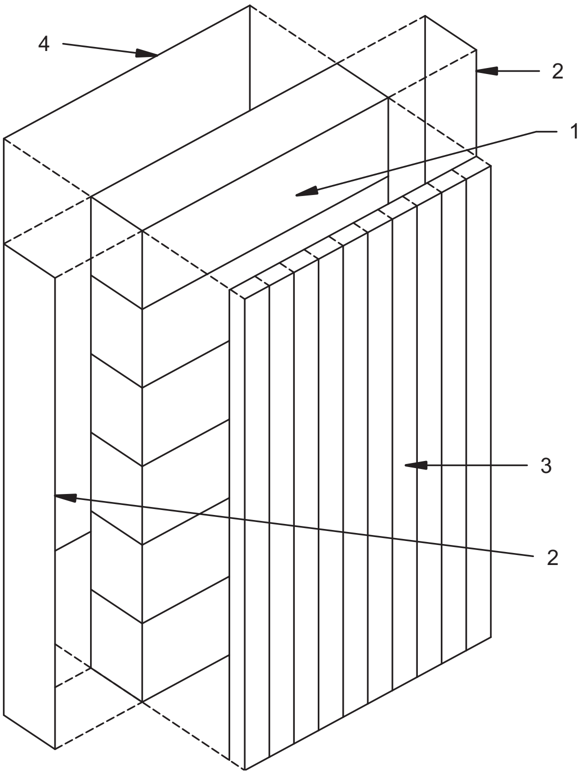


Fig. 5. Schematic of latent heat storage system: (1) aluminum PCM containers; (2) envelope of transparent polycarbonate; (3) tubes for fluid flow; and (4) wall for electric heater.

obtained by Voller [46] and for two-dimensional by Jiji [49]. In the model to see the effect of wall temperature on the melting rate, calculations have been made with 10 and 15 °C temperature. The following results were obtained:

(i) The effect of natural convection as melt fraction of PCM with time in one-dimensional model is more dominant as compared to melt fraction considering conduction only.
(ii) The effect of temperature difference between the wall and the melting point of PCM is more in convection mode of heat transfer.
(iii) The use of fins in two-dimensional case has increased the melt fraction about four times in comparison to the melt fraction without fins.

Saman and Vakilaltojjar [50] proposed a phase-change energy storage system as illustrated in Fig. 6 consisting of sections of different materials with different melting temperature for air conditioning applications. The PCMs are placed in thin flat plate containers and air is passed in series through gap in between them. PCM used are $CaCl_2 \cdot 6H_2O$ and potassium fluoride tetrahydrate ($KF \cdot 4H_2O$).

The freezing and melting processes of the PCM and heat transfer in the flowing fluid are unsteady two-dimensional problems for the system studied. To develop a mathematical

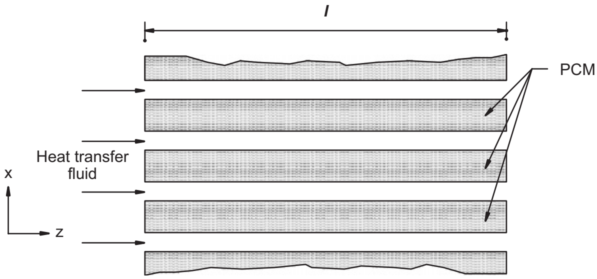


Fig. 6. Schematic diagram of the thermal energy storage system.

model assumptions made are:

1. PCM supercooling effects are neglected, axial conduction of the PCM and fluid are negligible.
2. The heat capacity of the fluid is ignored.
3. The quasi-static assumption is applied to convective heat transfer in the air passages, i.e. transient convection is considered as a series of steady-state problems.
4. The heat capacity and axial conduction of the container walls are negligible.
5. Natural convection in the liquid portion of PCM is ignored.

On the basis of these assumptions a mathematical model has been developed to predict the performance of storage system. In order to validate the additional assumptions, these assumptions are introduced into two subsequent models. The solidification of a liquid, initially at the melting temperature T_{m}, when the wall temperature is suddenly lowered to a value of T_{w} ($T_{\mathrm{w}} < T_{\mathrm{m}}$) is modeled. The same results can be obtained for the case of the melting process of a solid. In both cases melting and solidification process commences near the container wall. For a thermal storage system employing multiple PCMs, the calculation is carried out for the first material and then the outlet fluid temperature is used as the inlet fluid temperature for the second material and so on.

For model 1 the heat-transfer equation and the boundary and initial conditions for a PCM slab are as follows:

$$\frac{\partial T}{\partial t} = \alpha \frac{\partial^2 T}{\partial x_{\mathrm{w}}^2} \quad \text{for} \quad 0 < x_{\mathrm{w}} < \delta(t), \tag{10}$$

$$T_{x_{\mathrm{w}}=0} = T_{\mathrm{w}},$$
$$T_{x_{\mathrm{w}}=\delta(t)} = T_{\mathrm{m}}, \tag{11}$$

$$K \left.\frac{\partial T}{\partial x_{\mathrm{w}}}\right|_{x_{\mathrm{w}}=\delta} = \rho h_{\mathrm{f}} \frac{\mathrm{d}\delta}{\mathrm{d}t}.$$

The analytical solution of the above equation is known as the ‘‘Neumann Solution’’ and is presented by Carslaw et al. [51]. $\delta(t)$, $\mathrm{d}\delta/\mathrm{d}t$, T and the heat-transfer rate at the wall, q'' are calculated by the following equations:

$$\delta = 2s\sqrt{\alpha t}, \tag{12}$$

$$\frac{d\delta}{dt} = \frac{2\alpha}{\delta} s^2, \tag{13}$$

$$\frac{T - T_w}{T_m - T_w} = \frac{\text{erf}(su)}{\text{erf}(s)}, \tag{14}$$

$$q'' = -2s^2 \exp(s^2) \frac{Kh_f}{C_p \delta}. \tag{15}$$

The parameter s depends on Stefan number, Ste, which is the ratio of sensible heat to latent heat of the PCM, given by

$$Ste = \sqrt{pis} \exp(s^2)\text{erf}(s). \tag{16}$$

In second model the difference between the inlet air temperature and the melting point of PCM is assumed low, so Stefan number and sensible heat of PCM are very small than its latent heat can be ignored. This assumption has been made in second model; therefore Eq. (16) is simplified to

$$Ste = 2s^2. \tag{17}$$

δ and T_w are calculated by using equations

$$\frac{d\delta}{dt} = \frac{q}{\rho h_f}, \tag{18}$$

$$T_w = T_m - \frac{q\delta}{K}. \tag{19}$$

This approximation eliminates the need for trial and error in solving Eqs. (13) and (15) for calculating s.

In the third model in addition to the assumptions made in model 2, the wall temperature at the PCM side is assumed to be equal to the melting point of the PCM, before the solid–liquid interphase surface reaches the centerline of the PCM slab, and after that, it is equal to the air temperature. This assumption eliminates calculation loops for guessing the wall temperature.

For computer calculations finite-element method for grid size 30×30 is taken where 30 is the number of distance increments and next 30 is the number of time increments. Outlet air temperatures were calculated by applying different models and it is found that the temperature values of model 1, 2 and 3 have little difference, so model 3 is used in the subsequent calculations for variation of molten PCM layer thickness, wall temperature, slab thickness and air gap on the storage performance of thermal storage system. The results show that the air velocity profile at the entrance does not affect the heat-transfer characteristics and the outlet air temperature considerably. Better performance can be obtained by using smaller air gaps and thinner PCM slabs; however, this increases the number of PCM containers and the total volume of the storage system and will lead to higher pressure drop across the storage system.

Zhang et al. [52] gave a general model for analyzing the thermal performance of both melting and solidification process of latent heat thermal energy storage systems (LHTES) composed of PCM capsules. The model can be used to analyze the instantaneous

temperature distribution, instantaneous heat-transfer rate and thermal storage capacity of LHTES system. The model makes following assumptions to simplify the analysis:

- The physical properties of the PCM in both the liquid and solid phases are constant.
- Axial conduction in the PCM is negligible, $Ste \ll 1$, which means that the sensible heat can be neglected compared with latent heat in the PCM.
- The flow of HTF is fully developed.
- The convective heat-transfer coefficient between the HTF and the capsule is constant.

Zhang et al. [52] found that the thermal performance of a given system can be determined if $\overline{V_p} = f(Fo\theta_s)$ for a PCM capsule is known under given geometric and flow conditions i.e. (NTU, *Bi*, *Ste*, *Ar*, *Pr*) of LHTES, where $\overline{V_p}$ = (solid PCM volume/capsule volume) and $Fo = (\alpha_p \cdot t/l_c^2)$, where t is the time and l_c is the characteristic length of PCM capsule in meter. θ_s is dimensionless capsule surface temperature given by $[(T_s - T_{in})/(T_m - T_{in})]$.

Thus determination of $\overline{V_p} = f(Fo\theta_s)$ for a capsule is much easier than the determination of thermal performance for whole system. Relationships for $\overline{V_p} = f(Fo\theta_s)$ for some typical capsule geometries are available in the literature [14–17]. For solidification the model is validated with the results in literature where as thermal performance during melting is analyzed by taking example of LHTES composed of PCM spheres. In solidification it neglected the effect of density difference between solid and liquid PCM but considered this density variation during melting process. It showed that for the range of $0.5 < (\rho_l/\rho_s) < 1$ the melting rate reaches it's maximum when $\rho_l/\rho_s = 0.8$ and for the range of $1 < (\rho_l/\rho_s) < 1.10$ the melting rate increases with increasing ρ/ρ_s. The model is not limited to a specific system or a specific PCM, so it can be used to select and optimize system design and to stimulate the thermal behavior of LHTES.

Benmansour et al. [53] developed a two-dimensional numerical model that predicts the transient response of a cylindrical packed bed thermal energy storage system, which is randomly packed with spheres having uniform sizes and encapsulated the paraffin wax as a PCM and air as a working fluid flowing through the bed. The fluid energy equation was transformed by finite-difference approximation and solved by alternating direction implicit scheme, while the PCM energy equation was solved by using fully explicit scheme. The analysis is valid for fluids of various Prandtl number and it can be applied for both charging and recovery modes and for a broad range of Reynolds number. Measurements of both fluid and PCM temperatures were conducted at different axial and radial position and at different operating parameters. Experimental measurements of temperature distribution compare favorably with the numerical results over a broad range of Reynolds numbers and it shows that the effect of air mass flow rate on the bed temperature is quite apparent i.e. the time at which the bed reaches the thermal saturation state decreases significantly with the mass flow rate of air.

Xu et al. [54] developed a model to analyze the thermal performance of shape-stabilized PCM floor and studied the influence of melting temperature, heat of fusion, thickness of PCM layer and thermal conductivity of PCM on the thermal performance of passive solar buildings by using enthalpy model as it is simple in phase-change calculation and it takes enthalpy as the only variable instead of temperature and specific heat capacity. The shape stabilized PCM plate developed by author consists of 70 wt% paraffin on the dispersed PCM and 15 wt% polyethylene and 15 wt% styrene–butadiene styrene (SBS) block

copolymer as the supporting material. In order to simplify the analysis, the following assumptions were made:

- Heat transfer through walls, floor and ceiling is one dimensional.
- Thermo-physical properties of the building material are constant except the specific heat of PCM during melting or freezing process.
- The shape-stabilized PCM plate under surface is thermally insulated.

The simulative equations are solved numerically using the Gauss–Seidel method. A fully implicit finite-difference scheme was applied, and the number of grids was checked to ensure accuracy and to eliminate initial errors. The experimental and simulated results agree quite well.

In the analysis Xu et al. [54] found that to maintain indoor air temperature at comfortable level or for narrow indoor air temperature swing the suitable melting temperature of PCM should be roughly equal to the indoor air temperature of sunny winter days and the minimum heat of fusion and thermal conductivity should be 120 kJ/kg and 0.5 W/m K, respectively.

Halawa et al. [55] developed a two-dimensional model considering convection as a dominant mode to analyze the characteristics of a PCM thermal storage unit for roof integrated solar heating systems. In fact, the model presented is an improvement of the previous model used by Vakilaltjor [50]. The model takes into account the sensible heat transfer at the initial periods of melting and freezing of PCM and the inlet temperature of air is taken well above the melting point of the PCM which was not the case with previous model. However, both the models considered the variation of both the wall temperature and temperature of airflow alone the surface of wall. The mathematical model employed is based on enthalpy formulation and calculation of liquid fraction of PCM, sensible and total enthalpies when the PCM is in mushy zone is performed as per Voller [46]. In initial condition for the PCM melting process, the PCM is taken solid and its temperature is assumed at a certain value below the melting point. For freezing the PCM is initially liquid and its temperature is assumed at certain value above the melting point. These two situations can be expressed mathematically as

$$h_{\text{init}} = \rho_{\text{s}} c_{\text{s}} (T_{\text{m}} - T_{\text{init}}) \quad \text{for melting,} \tag{20}$$

$$h_{\text{init}} = \rho_{\text{l}} c_{\text{l}} (T_{\text{m}} - T_{\text{init}}) \quad \text{for freezing.} \tag{21}$$

The variation in wall and fluid temperatures along the air passage is taken care by using standard heat-transfer equations, for the duct cross-section at any distance x from the entrance, the following energy balance equation can be written as

$$m_{\text{a}} C_{pa}\, \mathrm{d}t/\mathrm{d}x = h_{\text{c}x} P (T_{\text{w}} - T_{\text{a}-x}) \tag{22}$$

The fluid mass flow rate m can be calculated from

$$m_{\text{a}} = \rho_{\text{a}} U_{\text{a}} A_{\text{f}}. \tag{23}$$

The heat conducted to the PCM surface node is given by

$$Q_{\text{cond}} = K_{\text{wall}} A_{\text{n}} \frac{T_{\text{wall}} - T_{\text{PCM}}}{\Delta y_{\text{wall}}}. \tag{24}$$

Eqs. (7)–(9) are used to calculate the fluid, wall and PCM surface node temperatures at any distance from the entrance. The surface node temperature, T_{PCM}, is used to determine

the sensible enthalpy, h_s, at the slab surface as follows:

$$h_s = \rho_s c_s (T_{PCM} - T_{Melt}), \quad T_{PCM} < T_{Melt}, \tag{25}$$

$$h_s = 0, \quad T_{PCM} = T_{Melt}, \tag{26}$$

$$h_s = \rho_l c_l (T_{PCM} - T_{Melt}), \quad T_{PCM} > T_{Melt}. \tag{27}$$

Halawa et al. [55] concluded that greatest heat-transfer rate occurs in the initial period of melting and freezing because of sensible heat transfer which will be advantageous in the heating of living space, where as next stage of melting/freezing occurs at relatively constant heat-transfer rate and the final stage of melting/freezing occurs at a very low heat-transfer rate, due to small temperature difference between the PCM and air. They stated that the constant temperature melting/freezing of PCM offers no additional benefit to the operation of PCM (TSU). Model validation is given in Saman et al. [56].

Sharma et al. [57] developed a two-dimensional theoretical model based on enthalpy approach considering mode of heat-transfer conduction only. Calculations were made to study the effect of thermal conductivity thermal capacity of fatty acids and conductivity of heat exchanger materials and their effect on melt fraction. The selected fatty acids were capric acid, lauric acid, myristic acid, palmitic acid and stearic acid and the heat exchanger material used were glass, stainless steel, tin, aluminum mixed, aluminum and copper were used as heat exchanger materials. Numerical solution of two-dimensional heat-transfer equation in the PCM based on enthalpy approach was carried out by using fully implicit finite-difference solution method. The boundary conditions used were the same as given by Costa et al. [45]. Following assumptions have been made to analyze the latent heat storage system.

- The thermo-physical properties of PCM's and fin material are independent of temperature but different for solid and liquid phases.
- The PCM is initially in solid phase.
- The PCM is homogeneous and isotropic.
- The mode of heat transfer is conduction only.

The performance of PCM storage system was analyzed by using a grid level of 32×32 (2×2 mm) with time step 20 s, where the grid level for the PCM was 30×30. The PCM was assumed 5 °C less than the melting temperature and the heating wall temperature was fixed at 15 °C higher than the melting temperature. The study converges to following conclusions:

(i) The thermal capacity of the container material has no significant effect on the melt fraction of PCM, having higher values of total enthalpy.
(ii) Thermal conductivity of container material and effective thermal conductivity of PCM have substantial effect on melt fraction.
(iii) The higher value of thermal conductivity of heat exchanger materials did not make significant contribution on the melt fraction of PCM.
(iv) Capric acid was found best PCM for latent heat storage system.
(v) Wall temperature difference has significant effect on the melt fraction of PCM.

However, this theoretical model is not validated against any experimental setup.

Anica Trp [58] analyzed the transient heat-transfer phenomenon during technical grade paraffin melting and solidification, in the shell and tube latent thermal energy storage system with water as HTF with moderate Prandtl number both numerically and experimentally. The mathematical model formulated to represent the physical system has been suited to treat both melting and solidification process. It has been based on following assumptions:

- The PCM is homogeneous and isotropic.
- The HTF is incompressible and it can be considered as a Newtonian fluid.
- Inlet velocity and inlet temperature of HTF is constant and its flow is laminar.
- Initial temperature of the latent heat storage unit is uniform and the PCM is in the solid phase for melting or in the liquid phase for solidification.
- Adiabatic outer wall is assumed.
- HTF, tube wall and PCM temperature variations in angular direction are assumed to be negligible i.e. the problem is two-dimensional.
- The problem is axisymmetric.
- Thermo-physical properties of the HTF the tube wall and PCM are constant.
- Natural convection in the liquid phase of PCM has been ignored.

The dimensionless transient fluid flow continuity, momentum and energy equations have been solved simultaneously with the tube wall and PCM energy equations. The enthalpy method for modeling phase-change heat transfer has been used. Governing conservation equations with initial and boundary conditions have been discretized by the control volume approach and the simple algorithm that was implemented in the self-written FORTRAN computer code and solved using an iterative procedure. Experimental investigations show that melting of used PCM occurs non-isothermally but with in the melting zone, on the other hand solidification occurs isothermally. The developed algorithm for non-isothermal melting has been implemented in numerical procedure. Numerical predictions for both melting and solidification agree quite well with experimental data. The result of numerical analysis show that the HTF velocity field reaches the fully developed condition quickly, while the temperature field never reaches a steady-state condition due to the moving melting and solidification fronts, therefore if a fluid with moderate Prandtl number such as water is used as HTF the heat transfer of HTF, the tube wall and the PCM has to solve as one domain by a numerical model that accounts for the thermal development region. The obtained numerical result give a good estimation of the phase-change material melting and solidification process which could provide guidelines for thermal performance and design optimization of the latent thermal energy storage unit.

Hed and Bellander [59] developed a mathematical model of the PCM air heat exchanger to show how the PCM heat exchanger unit can be modeled to fit into indoor climate and energy simulation software based on the finite-difference method, where the thermal properties of the material are considered and considerations are taken to different shapes of C_p (T) curve and it is shown that how the shape of C_p (T) curve will affect the cooling power of PCM heat exchanger.

The heat exchanger is modeled as duct with airflow where the PCM has a constant temperature. The equations for the heat balance for an element dx to calculate the power

of the heat exchanger is given by, see Fig. 7.

$$Q = vA\rho_a c_a(T(x) - T(x + dx) + P\,dx\,U_p(T_{PCM} - T(x)) = 0. \tag{28}$$

$$Q = vA\rho_a c_a(T_{in} - T(x)) = \alpha_p PL(T_{in} - T_{PCM}). \tag{29}$$

where α_p is fictive heat-transfer coefficient given by

$$\alpha_p = \frac{vA\rho_a c_a(1 - e((PU_pL))/(vA\rho_a c_a))}{PL}. \tag{30}$$

α_p can be compared with the surface heat-transfer coefficient and can be used when simulating the PCM–air heat exchanger unit in any simulation software. α_p is dependent of the geometry of the unit, the airflow and perimeter of the exposed material. After calculations it is found that the heat-transfer coefficient between the airflow and PCM increases significantly when the surface is rough as compared to smooth surface. In the design of a heat exchanger attention needs to be taken to the characteristics of the fan that drives the system. With high heat-transfer coefficient high power will be obtained for a short time where a low heat-transfer coefficient will yield a lower power for longer time. The effect of C_p (T) curve shows greatest difference between the ideal material and the materials where the heat transition takes place over a temperature span. In any design with PCM considerably attention needs to be taken to the time dependent behavior of the equipment, as there always be a limited amount of material available. To verify the calculations test runs were performed with the prototype heat exchanger at constant temperature. The inlet temperature is fed into the finite-difference model. The results of measurement and calculation agree quite well.

Dwarka and Kim [60] presented a mathematical model for comparing the thermal performance of randomly mixed and laminated PCM drywall system. The model was based on implicit enthalpy method and the governing equations for both randomly mixed and laminated PCM systems were solved by finite-difference method. The assumptions made for the model are:

- Both systems contain the same amount of PCM.
- One side of the wallboard is fully insulated.
- Air temperature is constant during the heat recovery and storage processes.
- Initial temperatures are the same through the board.

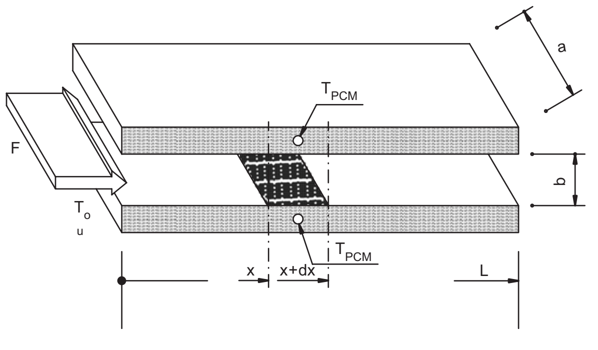


Fig. 7. Model for establishing the governing differential equation of the heat exchanger.

- There is no energy loss to surroundings.
- There is no convective heat transfer in the liquid phase of PCM.
- All thermo-physical properties are constant except the heat capacity.

For analysis of randomly mixed PCM systems the differential energy equation in rectangular coordinates (x, y and z) is represented as

$$\frac{\partial}{\partial x}\left(K\,\frac{\partial T}{\partial x}\right)+\frac{\partial}{\partial y}+K\left(\frac{\partial T}{\partial y}\right)+\frac{\partial}{\partial z}\left(K\,\frac{\partial T}{\partial z}\right)=\rho\,\frac{\partial h}{\partial t}=\rho\frac{\partial}{\partial t}\int C\,\mathrm{d}T, \tag{31}$$

where as for laminated PCM systems the general energy equation is reduced to one dimensional due to small relative thickness. The surface temperature variations for the samples were obtained through a series of computer simulations with different sets of thermo-physical properties and environmental conditions. The results showed a great advantage of the laminated PCM wallboard systems over the randomly mixed PCM types in terms of enhanced thermal performance and rapid heat-transfer rates under narrow temperature swing. For instance, the maximum instantaneous enhancement in heat flux was obtained between 20% and 50% higher during the phase-change process and up to about 18% more heat storage and release capacity. However, experimental evaluation is required towards validation and development of the laminated system.

4. Modeling based on second law of thermodynamics

Dessouky and Al-Juwayhel [61] presented a technique to predict the effect of different design and operating parameters on the entropy generation number or the second law effectiveness of a LHTES as shown in Fig. 8 consisting of heat storage and retrieval process, considering paraffin wax or $CaCl_2 \cdot 6H_2O$ as a phase-change material, where as the HTF considered was air or water. The system consists of a storage material with mass M. The latent heat of melting for the storage material is λ and the melting temperature is T_m. The storage material is contained in the annulus of a double-pipe heat exchanger. The

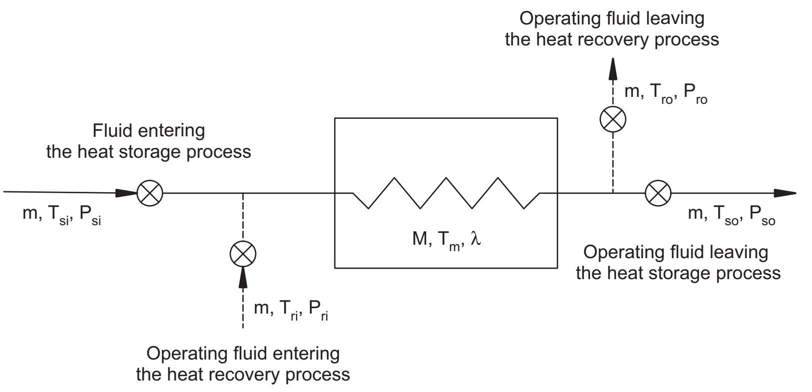


Fig. 8. Latent heat thermal energy storage system.

outer surface of the larger diameter tube is well insulated. The HTF, of mass M, flows inside the smaller diameter tube where it exchanges heat with the storage material. The system operates in a complete thermodynamic cycle, which consists of a heat storage process followed by a heat retrieval process. Through the storage process, the storage material changes phase from solid to liquid, while during the heat removal process, the material changes phase from liquid to solid. The phase change takes place at the constant melting temperature T_m.

The entropy generation number (N_s) is given by

$$N_s = \frac{T_a[(Sg)s + (Sg)r]}{W_s + W_r} \tag{32}$$

is determined as a function of the Reynolds's number of the operating fluid, specific heat-transfer area, operating fluid inlet temperature during the cyclic process of heat storage and retrieval processes and the thermo-physical properties of both the storage materials and the HTFs. The thermodynamic analysis presented was based on following assumptions:

- The heat storage material is always at its melting temperature during both the energy storage and retrieval processes.
- There is no heat exchange between the system and surroundings.
- The same working fluid, with a constant flow rate is used during both processes.
- Constant thermo-physical properties of both the storage materials and the working fluids.
- The resistance to heat transfer due to heat exchange wall is negligible.
- The enthalpy of working fluid is zero at 0 °C and its pressure leaving the system is atmospheric throughout the heat supply and removal processes.

The second law efficiency is related to the number of entropy generation units by the following equations:

$$\psi = 1 - N_s. \tag{33}$$

The application of developed analysis was demonstrated by considering a system, which consists of simple double pipe heat exchanger. The inner tube is made of commercial steel and the heat storage material is placed in the annulus of the heat exchange and the operating fluid exchanges heat with the systems during its flow through the interior tube. The conclusions drawn from the analysis are:

(i) The energy storage system using water wax has the maximum second law effectiveness.
(ii) The minimum second law efficiency is obtained from the air–$CaCl_2 \cdot 6H_2O$ system.
(iii) The second law effectiveness increases with the increase of Reynolds's number, specific heat-transfer area and operating fluid wall temperature in the heat recovery process and with the decrease of fluid inlet temperature in the heat storage process.
(iv) The dependency of the entropy generation number on the Reynolds's Number is more pronounced when water is the HTF.
(v) The water inlet temperature during the heat recovery process has a very low impact on the entropy generation number.

Gong et al. [62] developed a physical model of the latent heat thermal storage system consists of a PCM and a HTF. The fluid flows through the PCM to store or extract energy. During the energy charge process hot fluid flows through the PCM and the thermal energy conveyed by the fluid is stored in the PCM. During the energy discharge process cold fluid flows through the PCM to extract the thermal energy stored in the PCM and delivers it to the user. To facilitate the analysis a lumped model for the PCM and a distributed model for the HTF are employed. The lumped model assumes that the PCM is a reservoir with a constant temperature of its melting point. The distributed model assumes that the temperature of the HTF varies only along its flow direction with the heat transferred into or out of the HTF. An actual system of this sort is characterized by the thermo-physical properties of the PCM, the geometry and the size of the storage module, the thermo-physical properties of the HTF, as well as the operating conditions such as fluid inlet temperatures and fluid flow rate. Under the assumption of the lumped model for the PCM, the sensible heat effects are neglected and consequently the outlet temperatures of the HTF are time-independent.

A thermodynamic analysis of a thermal energy storage system employing multiple PCMs is developed. Relative merits of a thermal exergy storage systems using two, three as well as five PCMs are investigated. It is discovered that the energy efficiency can be significantly improved using multiple PCMs compared with a single PCM in a system. Optimizations of the melting points for the two, three and five PCM systems are performed. The exergy efficiency of the charge process, defined as the ratio of the exergy rate stored in the PCM and the total exergy rate possessed by the HTF before contact with the PCM for a single PCM system is given by

$$\beta_{\mathrm{c}}^{1}=\frac{W_{\mathrm{c}}^{1}}{W_{\mathrm{T}}}=\frac{(1-\mathrm{e}^{-N_{\mathrm{c}}})(T_{\mathrm{ci}}-T_{\mathrm{m}})(1-(T_{\mathrm{a}}/T_{\mathrm{m}})}{T_{\mathrm{ci}}-T_{\mathrm{a}}-T_{\mathrm{a}}\ln(T_{\mathrm{ci}}/T_{\mathrm{a}})}. \tag{34}$$

The exergy efficiency of the discharge process, defined by the ratio of the rate of exergy gain of the HTF and the rate of exergy release by the PCM through the discharge process for a single PCM system is given by

$$\theta_{\mathrm{d}}^{1}=\frac{\omega_{\mathrm{d}}^{1}}{\omega_{\mathrm{Td}}^{1}}=\frac{\theta_{\mathrm{do}}^{1}-\theta_{\mathrm{di}}-\ln(\theta_{\mathrm{do}}^{1}/\theta_{\mathrm{di}})}{(1-\mathrm{e}^{-N_{\mathrm{d}}})(\theta_{\mathrm{m}}-\theta_{\mathrm{di}})(1-(1/\theta_{\mathrm{m}})}. \tag{35}$$

From the analysis it is noted that the overall exergy efficiency of a thermal storage system varies with the number of PCMs used in the system, the number of the heat-transfer units of the storage exchanger as well as the inlet temperatures in both the charge and discharge processes. The analytical results provide guidance in the selection of appropriate number of PCMs and the PCMs, which have appropriate melting points to maximize the system efficiency in practical design of thermal storage systems. For the first time it is shown that the exergy efficiency of the storage system can be doubled or even almost tripled when using three or five PCMs. This analysis is limited to only latent heat effects and to the optimization of the melting points of the PCM; other thermo-physical properties of course have effects on the system performance. Further refinement of this analysis should include the effects of sensible heat and other thermo-physical properties of the PCMs for the charge/discharge cycle.

Table 6
Comparison of different models used for LHTES systems using PCM

Model name	Dimensional	Thermo-physical properties	Geometry	Steady/ transient	Model verification	Utility
Models based on first law of thermodynamics						
Shamsunder et al. [32]	Multi-dimensional	Constant (except enthalpy of PCM) independent of temperature	Square container	Transient	Model is verified by numerical experiments and shows good agreement	Model is general and powerful to apply successfully to the wide range of problems
Hamdan et al. [33]	Two dimensional	n.a.	Rectangular	n.a.	Model shows good agreement with the experimental work carried by other researchers	This model can be used to predict melting rate and the amount of thermal energy stored with in a storage system containing a PCM
Kurkulu et al. [37]	Two dimensional	Constant	Square cross-section	n.a.	Model is verified with experimental results and agrees well	Model can be used to analyze the thermal performance of PCM storage
Esen et al. [38]	Two dimensional	Constant	Cylindrical	Transient	Model is verified with experimental results	Model can be useful to optimize the performance of solar-assisted cylindrical energy storage tank by careful selecting PCM
Gong et al. [41]	Two dimensional	Constant	Cylindrical	Transient	n.a.	Model analyzes guidance for selection of hot and cold fluid. Analysis is limited to only conduction controlled melting/ freezing heat transfer in the PCM
Costa et al. [45]	One dimensional without fins and two dimensional with fins	Constant	Rectangular	Transient	Model is verified against numerical tests and shows good agreement	Model can be used to design a latent heat thermal energy storage system to take advantage of the off peak electrical energy foe space heating

Saman and Vakilaltojjar [50]	Two dimensional	Constant	Rectangular	Transient	Not verified	Model can be used for air-conditioning applications
Zhang et al. [52]	One dimensional	Constant	Spherical capsule	Transient	For solidification process model is validated with the results in literature and agrees well	Model can be used to select and optimize system design and the thermal behaviour of latent heat thermal energy storage systems
Benmansour et al. [53]	Two dimensional	Constant	Spherical capsule	Transient	Model is verified with experimental results and agrees well	Model used to predict the response of a cylindrical packed bed thermal energy storage system and analysis is valid for broad range of Prandtl and Reynolds number
Xu et al. [54]	One dimensional	Constant (except specific heat of PCM)	Shape stabilized PCM floor	Transient	Model is verified with experimental results and agrees well	Model is helpful for the application of shape stabilized PCM floor in solar energy buildings
Halawa et al. [55]	Two dimensional	Constant	Rectangular	Transient	Model is verified against number of experimental data and agrees well	Model is helpful in developing a PCM thermal storage unit (TSU) of a roof integrated solar heating system and to analyse the characteristics of PCM TSU
Sharma et al. [57]	Two dimensional	Constant (except in solid and liquid phases of PCM)	Heat exchanger	Transient	Not verified	Model is helpful in predicting interface profile of the PCM and assists in selection of design parameter of heat exchanger
Trp [58]	Two dimensional	Constant (except specific heat)	Shell and tube	Transient	Model is verified against experimental set up and shows good agreement	The model provides guidelines for shell- and tube-type LHTES performance and design optimization
Hed and Bellander [59]	One dimensional	Constant (except specific heat)	Rectangular	n.a.	Model is verified against experimental set up and shows good	Model gives a method to simulate a PCM air heat exchanger and it can be developed to fit into a finite

Table 6 (*continued*)

Model name	Dimensional	Thermo-physical properties	Geometry	Steady/ transient	Model verification	Utility
					agreement except the end temperature which is due to difficulty in measurements of air flow	difference based indoor climate & energy simulation software
Dwarka and Kim [60]	Three dimensional (for randomly mixed PCM) One dimensional (for laminated PCM)	Constant except heat capacity	Wallboard	n.a.	Not validated	Model is useful in assessment of inadequate heat transfer and overall reduction of thermal conductivities during energy recovery mode of PCM wall board systems
Models based on second law of thermodynamics						
Dessouky and Al-Juwayhel [61]	n.a.	Constant	Cylindrical tube	n.a.	Not validated	The model is helpful in predicting the effect of different design and operating parameters on the entropy generation number or the second law effectiveness of a heat storage system using PCM
Gong et al. [62]	n.a.	Constant	n.a.	Transient	Not validated	The model provides guidance in the selection of appropriate number of PCM's which have appropriate melting points to maximize the system efficiency in practical design of thermal storage systems

n.a.: not available.

5. Discussions

Table 6 shows the comparison of different models used in PCM for latent thermal energy storage systems. All the models have their specific utility for which these models had been verified with experimental results. Most of the models based on first law of thermodynamics are verified and ensures good agreement with experimental results but the model based on second law of thermodynamics are not verified against any experimental set up, which puts a question mark on their acceptability. To prove the acceptability of these models some experimental exercise should be done.

6. Conclusions

Latent heat thermal energy storage systems are used for the storage of excess energy available by the solar or any other sources. There are many methods for the energy storage but the latent heat thermal energy storage is good among all the storage systems. In this work, a review of the present state of mathematical modeling under two different categories is given. One, on the basis of first law of thermodynamics and the other is second law of thermodynamics. There are many researchers who have worked on first law of thermodynamics and most of them verified their results by experimental investigations, which prove their acceptability. In contrast to first law a very little work has been done on the second law of thermodynamics. The second law (exergy) analysis develops a good understanding of the thermodynamic behavior or efficiency of thermal energy storage system contrary to first law of thermodynamics, as it does not take into account the time duration by which heat is supplied. There is requirement of some experimental work by which the acceptability of second law analysis can be substantiated.

References

[1] Hasnain SM. Review on sustainable thermal energy storage technologies, Part 1: heat storage materials and techniques. Energy Convers Manage 1998;39:1127–38.
[2] Duffie JA, Beckman WA. Solar engineering of thermal processes. New York: Wiley; 1991.
[3] Gibbs BM, Hasnain SM. DSC study of technical grade phase change heat storage materials for solar heating applications. In: Proceedings of the 1995 ASME/JSME/JSEJ international solar energy conference, Part 2, 1995.
[4] Telkes M. Thermal storage for solar heating and cooling. In: Proceedings of the workshop on solar energy storage subsystems for the heating and cooling of buildings, Charlottesville, Virginia, USA, 1975.
[5] Pillai KK, Brinkworth BJ. The storage of low-grade thermal energy using phase change materials. Appl Energy 1976;2:205–16.
[6] Telkes M. Thermal energy storage in salt hydrates. Solar Energy Mater 1980;2:381–93.
[7] Wood RJ, et al. In: Proceedings international conference energy storage, Brighton, UK, 1981, p. 145.
[8] Heine D, Abhat A. In stat: mankind's future source of energy, vol. 500. NY, USA; Pergamon Press; 1978.
[9] Carlsson B, Wettermark G. Heat transfer properties of a heat of fusion store based on $CaCl_2 \cdot 6H_2O$. Sol Energy 1980;24:239–47.
[10] Lane GA. Solar heat storage: latent heat materials, vol. 1. USA: CRC Press Inc.; 1983.
[11] Hasnain SM. PhD dissertation, Department of Fuel and Energy, University of Leeds, UK, 1990.
[12] Abhat A. Low temperature latent heat thermal energy storage: heat storage materials. Sol Energy 1983;30:313–32.
[13] Zalba B, Ma Marın J, Cabeza Luisa F, Mehling H. Review on thermal energy storage with phase change: materials, heat transfer analysis and applications. Appl Therm Eng 2003;23:251–83.

[14] Farid MM, Khudhair AM, Razack SAK, Al-Hallaj S. A review on phase change energy storage: materials and applications. Energy Convers Manage 2004;45:1597–615.
[15] Jotshi CK, Goswami DY, Tomilnson JJ. In: Proceedings of 1992 ASES annual conference, USA, 1992.
[16] Garg HP, Mullick AC, Bhargava AK. Solar thermal energy storage. Dordrecht: D. Reidel Publishing Company; 1985 [p. 241–242][Title TJ810.G349].
[17] Naumann R, Emons HH. Results of thermal analysis for investigation of salt hydrates as latent heat-storage materials. J Therm Anal 1989;35:1009–31.
[18] Hawes DW, Feldman D, Banu D. Latent heat storage in building materials. Energy Buildings 1993;20:77–86.
[19] Nagano K, Mochida T, Iwata K, Hiroyoshi H, Domanski R. Thermal performance of $Mn(NO_3)_2 \cdot 6H_2O$ as a new PCM for cooling system. In: Fifth workshop of the IEA ECES IA, Tsu (Japan), 2000 [Annex 10].
[20] Li JH, Zhang GE, Wang JY. Investigation of a eutectic mixture of sodium acetate trihydrate and urea as latent heat storage. Sol Energy 1991;47(6):443–5.
[21] Dincer I, Rosen MA. Thermal energy storage, systems and applications. Chichester (England): Wiley; 2002.
[22] Belton G, Ajami F. Thermochemistry of salt hydrates. Report no. SF/RANN/SE/GI27976/TR/73/4, Philadelphia (Pennsylvania, USA), 1973.
[23] Lane GA. Low temperature heat storage with phase change materials. Int J Ambient Energy 1980;1:155–68.
[24] Sasaguchi K, Viskanta R. Phase change heat transfer during melting and re-solidification of melt around cylindrical heat source(s)/sink(s). J Energy Resour Technol 1989;111:43–9.
[25] Schroder J. Thermal energy storage and control. J Eng Ind 1975;97:893–6.
[26] Wada T, Kimura F, Yamamoto R. Studies on salt hydrates for latent heat storage, II: eutectic mixture of pseudo binary system $CH_3CO_2Na \cdot 3H_2O$–CO $(NH_2)_2$. Bull Chem Soc Japan 1983;56:1223–6.
[27] Bejan A. Two thermodynamic optima in the design of sensible heat units for energy storage. J Heat Transfer Trans ASME 1978;100:708–12.
[28] Krane RJ. A second law analysis of the optimum design and operation of thermal energy storage systems. Int J Heat Mass Transfer 30(l); 43–57.
[29] Bejan A. Advanced engineering thermodynamics. New York: Wiley; 1988.
[30] Krane RJA. Second law analysis of a thermal energy storage system with Joulean heating of the storage element. In: Proceedings of the ASME, WA-HT-19, Miami Beach, FL, 1985. p. 1–10.
[31] Adebiyi GA, Russell LD. Second law analysis of phase-change thermal energy storage systems. In: Proceedings of the ASME, WA-HTD-80, Boston, MA, 1987, p. 9–20.
[32] Shamsundar N, Sparrow EM. Analysis of multidimensional conduction phase change via the enthalpy model. J Heat Transfer Trans ASME 1975;97:333–40.
[33] Hamdan MA, Elwerr FA. Thermal energy storage using a phase change material. Sol Energy 1996;56(2): 183–9.
[34] Elwerr F. New mathematical analytical method for solving phase-change problems. MS thesis, University of Jordan, 1993.
[35] Benard C, Gobin G, Martinez F. Melting in rectangular enclosures: experiments and numerical simulations. J Heat Transfer Trans ASME 1985;107:794–802.
[36] Webb B, Viskanta R. Analysis of heat transfer during melting of a pure metal from an isothermal vertical wall. Numer Heat Transfer 1986;9:539–58.
[37] Kurkulu A, Wheldon A, Hadley P. Mathematical modelling of the thermal performance of a phase-change material (PCM) store: cooling cycle. Appl Therm Eng 1996;16(7):615–23.
[38] Esen M, Ayhan T. Development of a model compatible with solar assisted cylindrical energy storage tank and variation of stored energy with time for different phase change materials. Energy Convers Manage 1996;37(12):1775–85.
[39] Visser H. Energy storage in phase-change materials—development of a component model compatible with TRNSYS, Final report, Contract no. 2462-84-09 ED ISPNL, Delft University of Technology, Department of Applied Physics, Delft, 1986.
[40] Esen M. Numerical simulation of cylindrical energy storage tank containing phase change material on the solar assisted heat pump system and comparing with experimental results. Doctoral thesis, Department of Mechanical Engineering, Karadeniz Technical University, Trabzon, Turkey, 1994.
[41] Gong ZX, Mujumdar AS. Finite-element analysis of cyclic heat transfer in a shell-and-tube latent heat energy storage exchanger. Appl Therm Eng 1997;17(6):583–91.
[42] Zienkiewicz OC, Taylor RL. The finite element method. London: McGraw-Hill; 1989.
[43] Dalhuijsen DJ, Segal A. Comparison of finite element techniques for solidification problems. Int J Numer Methods Eng 1986;23:1807–29.

[44] Pham QT. The use of lumped capacitance in the finite-element solution of heat conduction problems with phase change. Int J Heat Mass Transfer 1986;29:285–91.
[45] Costa M, Buddhi D, Oliva A. Numerical simulation of a latent heat thermal energy storage system with enhanced heat conduction. Energy Convers Manage 1998;39(3–4):319–30.
[46] Voller VR. Fast implicit finite difference method for the analysis of phase change problems. Numer Heat Transfer Part B 1990;17:155.
[47] Patankar SV. Numerical heat transfer and fluid flow. Washington, DC: Hemisphere Publishing Corporation; 1980.
[48] Goodrich L. Efficient numerical technique for one-dimensional thermal problems with phase change. Int J Heat Mass Transfer 1978;21:615–21.
[49] Rathjen KA, Jiji LM. Heat conduction with melting or freezing in a corner. J Heat Transfer 1971;93:101–9.
[50] Vakilaltojjar SM, Saman W. Analysis and modeling of a phase change storage system for air conditioning applications. Appl Therm Eng 2001;21:249–63.
[51] Carslaw HS, Jaeger JC. Conduction of heat in solids. London, Oxford: Clarendon Press; 1959.
[52] Zhang Y, Su Yan, Zhu Y, Hu X. A General model for analyzing the thermal performance of the heat charging and discharging process of Latent heat thermal energy storage systems. Trans ASME J Sol Energy Eng 2001;123:232–6.
[53] Benmansour A, Hamdan MA, Bengeuddach A. Experimental and numerical investigation of solid particles thermal energy storage unit. Appl Therm Eng 2005, in press.
[54] Xu X, Zhang Y, Lin K, Di H, Yang R. Modeling and simulation on the thermal performance of shape-stabilized phase change material floor used in passive solar buildings. Energy Buildings 2005;37:1084–91.
[55] Halawa E, Bruno F, Saman W. Numerical analysis of a PCM thermal storage system with varying wall temperature. Energy Convers Manage 2005;46:2592–604.
[56] Saman W, Bruno F, Halawa E. Thermal performance of PCM thermal storage unit for a roof integrated solar heating system. Sol Energy 2005;78(2):341–9.
[57] Sharma A, Wona LD, Buddhi D, Parka JU. Technical note: numerical heat transfer studies of the fatty acids for different heat exchanger materials on the performance of a latent heat storage system. Renew Energy 2005;30:2179–87.
[58] Trp A. An experimental and numerical investigation of heat transfer during technical grade paraffin melting and solidification in a shell-and-tube latent thermal energy storage unit. Sol Energy 2005;79:648–60.
[59] Hed G, Bellander R. Mathematical modelling of PCM air heat exchanger. Energy Buildings 2006;38:82–9.
[60] Dwarka K, Kim JS. Thermal analysis of composite phase change drywall systems. Trans ASME J Sol Energy Eng 2005;127:352–6.
[61] El-Dessouky H, Al-Juwayhel F. Effectiveness of a thermal energy storage system using phase-change materials. Energy Convers Manage 1997;38(6):601–17.
[62] Gong ZX, Mujumdar AS. Thermodynamic optimization of the thermal process in energy storage using multiple phase change materials. Appl Therm Eng 1997;17(2):1067–83.